Available online at www.sciencedirect.com

ScienceDirect

Solar Energy 125 (2016) 51–64

SOLAR ENERGY

www.elsevier.com/locate/solener

Fast and quick degradation properties of doped and capped ZnO nanoparticles under UV–Visible light radiations

Manish Mittal [a], Manoj Sharma [b,1], O.P. Pandey [a,*]

[a] School of Physics and Materials Science, Thapar University, Patiala 147002, Punjab, India
[b] Department of Nanotechnology, Sri Guru Granth Sahib World University, Fatehgarh Sahib 140406, Punjab, India

Received 15 August 2015; received in revised form 25 November 2015; accepted 6 December 2015
Available online 28 December 2015

Communicated by: Associate Editor Gion Calzaferri

Abstract

Undoped and Manganese (Mn) doped zinc oxide (ZnO) ($Zn_{1-x}Mn_xO$, $x = 0.005$, 0.01, 0.015 and 0.02) nanoparticles (NPs) capped with (1.0%) Thioglycerol (TG) has been successfully synthesized by co-precipitation method. Optical and morphological studies have been done for photophysical and structural analysis of synthesized materials. The photocatalytic activity of undoped and Mn doped ZnO NPs were investigated by degradation of crystal violet (CV) dye under UV–Visible light radiations. It has been found that Mn (1.0%) doping concentration is optimal for photophysical and photocatalytic properties. When the pH of as synthesized optimum doped ZnO NPs varied from natural pH i.e. from 6.7 to 8.0 and 10.0, the degradation of CV dye increases from 92% to 95% and 98% in 180 min respectively. Further on increasing the pH of optimum doped synthesized NPs to 12.0, almost 100% degradation has been achieved in 150 min. Optimum doped photocatalyst synthesized at pH-12.0 has also effectively degraded the CV dye solution in acidic and basic medium thus showed its utility in various industries. However, it has been found that 100% of CV dye quickly degraded in 30 min when only 1.0% of hydrogen peroxide (H_2O_2) was introduced along with optimized NPs synthesized at pH-12. Kinetic studies show that the degradation of CV dye follows pseudo first and second-order kinetic law. Further an industrial anionic polyazo Sirius red F3B (SRF3B) dye has been degraded to 100% with optimized NPs synthesized at pH-12.0 in 15 min only.

Keywords: ZnO; Photocatalytic degradation; Nanoparticles; Doping; pH

1. Introduction

With increasing diversity in industrial products environmental problems related to industrial effluents are becoming more and more complex. The residual dyes from different sources like textile industries, pharmaceutical industries, bleaching industries, dyeing, paper and pulp industries etc. introduces a variety of organic pollutants into natural resources of water. Such dye effluents pose a major threat to the surrounding ecosystem owning to their toxicity, non-biodegradability and even may cause cancer or mutagenic to life (Lima et al., 2015). These dyes remain in water for long time without adequate treatment. Various processes such as flocculation, adsorption, ultra-filtration, precipitation and reverse osmosis are applied to remove toxic substances generated from dyes in wastewater. However, using these processes highly concentrated pollutant phases are generated (Akyol and Bayramoglu, 2005). Recently, semiconductor based photocatalytic degradation

* Corresponding author. Tel.: +91 175 2393130 (O), +91 9888401777 (mobile).
E-mail address: oppandey@thapar.edu (O.P. Pandey).
[1] Presently at UNAM–Institute of Materials Science and Nanotechnology, Bilkent University, Ankara 06800, Turkey.

http://dx.doi.org/10.1016/j.solener.2015.12.003
0038-092X/

of dyes has attracted more attention because it is able to oxidize low concentration of organic pollutants into non toxic products (Kislov et al., 2009). It is generally accepted that, when semiconductor absorbs a photon with energy greater than or equal to band gap energy of semiconductor, an electron is excited from filled valence band to empty conduction band, leaving a hole in the valence band. If suitable trap states created by defects or by dopant are available to trap these photo-generated electrons and holes, recombination is prevented and thus they can be used to perform redox reactions. Hole lying in the valence band react with the surface bound H_2O or OH^- to produce powerful oxidizing agent such as hydroxyl radical. On the other hand, the electron in the conduction band reacts with dissolved oxygen species to generate superoxide anion radicals, which are again highly reactive for oxidizing organic compounds (Akpan and Hameed, 2009). Till now, many kinds of semiconductors have been studied as photocatalysts such as TiO_2, ZnO, ZnS, WO_3, and CdS (Rehman et al., 2009; Sharma et al., 2012; Bhosale et al., 2014; Chandran et al., 2014). TiO_2 is the most widely used effective photocatalyst for its high efficiency, non-toxic nature, low cost and photochemical stability. To significantly improve the photocatalytic efficiency of TiO_2, it has been doped with Au, Fe (III), Co, Al^{3+}, V etc. (Kamat, 2002; Martin et al., 2004; Chio et al., 1994; Klosek and Raftery, 2001). It has been found that on doping with Au and Fe (III) in TiO_2 increases the photocatalytic efficiency by small amount but doping Co and Al^{3+} has inverse effect on photo-reactivity of TiO_2. However, V^- doped TiO_2 showed better photo-reactivity but the by-products were carbon monoxide and formic acid which are also toxic in nature. On the other hand ZnO has been found to be better alternative to TiO_2 because of its higher reaction and mineralization rates and also it generates oxidizing agents more efficiently (Behnajady et al., 2006; Poulios et al., 1999). Biggest advantage of ZnO over TiO_2 is that it absorbs larger fraction of UV spectrum and its corresponding threshold is 425 nm. Since the contaminant molecules need to be adsorbed on the surface of photocatalyst before the photocatalytic reaction takes place, the surface area and crystal defects play a significant role in the photocatalytic activity. Doping of metal oxide with transition metal ions improve the photocatalytic activity by increasing the crystal defects and tailoring the band gap energies to shift the optical absorption toward visible region (Wang et al., 2013). Mn doped ZnO shows better degradation in visible region as Mn doping creates defect states which act as the intermediate steps for the electrons to excite from valence band to the conduction band (Wang et al., 2013; Mahmood et al., 2011). To the best of our knowledge, in most of the studies pH of the dye has been varied with the addition of acids or bases to make it cationic or anionic without varying the pH of as synthesized semiconductor photocatalyst (Ji et al., 2009; Kong et al., 2010). We have already reported the effect of pH of as synthesized Cu doped ZnO NPs on photocatalytic activity (Mittal et al., 2014). Till date, no study has been done on the effect of pH of as synthesized Mn doped ZnO NPs on photocatalytic degradation studies. In the present work, nanosized undoped and manganese (Mn) doped with TG capped ZnO NPs were prepared by co-precipitation route at different pH. These synthesized NPs were used as a photocatalyst to study the photocatalytic degradation of CV dye as a model of organic compound under UV–Visible irradiations. The effect of doping concentration and pH has been studied in detail. The results confirm that Mn doped ZnO NPs synthesized at higher pH values show enhanced UV–Visible light induced degradation of CV dye. Further the addition of 1.0% H_2O_2 to optimum doping concentration of as synthesized Mn doped ZnO NPs at pH-8.0, 10.0 and 12.0, fast and quick degradation of CV dye has been observed. The photocatalytic results so obtained are contradictory to others who reported that Cu and Mn doped ZnO NPs show nearly same or lesser photocatalytic activity than undoped ZnO NPs (Milenova et al., 2013; Donkova et al., 2010).

2. Experimental section

For these studies chemicals of analytical grade were purchased from Sigma Aldrich. ZnO NPs were synthesized by chemical co-precipitation method (Mittal et al., 2014). In the first step 40 mL homogeneous solution of 0.5 M zinc acetate, (1.0%) (at. wt.) TG and 0.5 M sodium hydroxide were prepared in distilled water separately by stirring them for half an hour. For the synthesis of undoped and capped ZnO NPs, 1.0% TG solution was added to the 40 mL solution of 0.5 M zinc acetate in aqueous medium. After half an hour 0.5 M sodium hydroxide was added dropwise to the above solution. Soon after the addition of sodium hydroxide the precipitation phenomenon occurs and the concentration of precipitates increases as the addition was increased. Sodium hydroxide was added into the solution till the pH of the solution reaches to 8.0. The stirring was allowed for another half an hour. For synthesis of Mn (0.5%) doped and TG (1.0%) capped ZnO NPs at pH-8.0, 40 mL homogeneous solution of 0.5 M zinc acetate and 40 mL solution of 0.5 M sodium hydroxide was prepared. 40 mL homogeneous solution of 0.5 M manganese acetate and TG solution of 1.0% (at. wt.) each were prepared in distilled water separately with constant stirring for half an hour. Firstly (0.5%) manganese acetate solution was added dropwise to 40 mL zinc acetate solution and then TG (1.0%) was added to same solution. After stirring of about half an hour sodium hydroxide solution was added dropwise till the pH of the solution reaches to 8.0. The stirring was allowed for another half an hour. For synthesis of Mn (1.0%, 1.5% & 2.0%) doped and TG (1.0%) capped ZnO NPs at pH-8.0 and Mn (1.0%) doped and TG (1.0%) capped ZnO NPs at pH-10.0 and 12.0, similar procedure was adopted. The capping agent was used for avoiding agglomeration. Different solutions containing TG (1.0%) capped undoped and Mn (0.5%, 1.0%, 1.5% and

2.0%) doped ZnO NPs synthesized at pH-8.0 and Mn (1.0%) doped capped NPs synthesized at pH-10.0 and 12.0 were then centrifuged at 10,000 rpm for 5 min. The precipitated particles were filtered using Whatman-40 filter paper. The particles were washed several times to remove the last traces of adhered impurities. The wet powders were dried at 70 °C in vacuum oven for 24 h. Finally, the powders were calcined at 300 °C for 3 h to produce the nano sized doped and capped ZnO powder.

2.1. Characterization

The ZnO NPs were characterized by X-ray diffraction (XRD) technique using Panalytical Xpert Pro MPD diffractometer with Cu (Kα) radiations. The ZnO NPs were characterized using Hitachi (H-7500) Transmission electron microscope (TEM) operating at 80 kV. Samples for TEM studies were prepared by dispersing the NPs in ethanol and placing a drop of nano dispersed powder on a carbon coated Cu grid. The solvent was allowed to evaporate at room temperature. Optical absorption spectra of ZnO NPs was recorded with double beam UV–Visible spectrophotometer using Hitachi U-3900H in the range 300–650 nm. For this 0.001 gm sample was dispersed in 5 mL of distilled water and further ultrasonicated for half hour to obtain transparent colloidal solutions. PL excitation and emission spectra of powdered sample has been recorded with Edinburgh Instruments FS920 spectrometer equipped with 450 W Xenon Arc Lamp and a cooled single photon counting photomultiplier (Hamamatsu R2658P).

2.2. Photo reactor and experimental procedure

A photo reactor was designed and fabricated in our laboratory for photo degradation studies (Mittal et al., 2014). It contains three jackets. At the innermost jacket of cylindrical vessel a mercury lamp was placed which had broad emission range. The middle jacket was surrounded by circulating water intended to control the temperature during the reaction. Solution of CV dye and prepared ZnO catalyst was placed in the outermost jacket and whole apparatus was then placed on the magnetic stirrer which can work on variable temperature and rpm. Here all experiments were performed at room temperature and at 1500 rpm. The photocatalytic reaction was carried out with 0.25 g ZnO nanopowder suspended in 100 mL of dye solution (crystal violet). The concentration of the dye used for photocatalytic degradation was 10 mg/L. At different time intervals the slurry (dye and ZnO nanopowder) was sampled and centrifuged at 10,000 rpm and then supernatants were analyzed by the UV–Visible spectrophotometer to study the photocatalytic degradation of CV dye. All the experiments have neutral pH of CV dye solution even after the addition of photocatalysts synthesized at different pH. However, to check the photocatalytic efficiency and utility of synthesized NPs at higher pH values in industries, degradation of CV dye has been studied by varying the pH of CV dye solutions at pH-2.0 and 10.0.

3. Results and discussion

3.1. XRD – studies

The XRD pattern of TG (1.0%) capped undoped and Mn (0.5–2.0%) doped ZnO NPs synthesized at natural pH is shown in Fig. 1. The diffraction peaks corresponding to (100), (002), (101), (102), (110), (103), (200), (112) and (201) planes reveals a highly crystalline hexagonal wurtzite structure (JCPDS No. 36-1451). There is no extra peak corresponding to Mn, oxides of Mn or Mn related secondary and impurity phases in Fig. 1 confirming that manganese has been incorporated to ZnO lattice rather than interstitial ones. The average crystallite size is estimated by Debye–Scherer formula

$$D = 0.9\lambda/\beta\cos\theta \quad (1)$$

where D is crystallite size (in nm), 'λ' is the wavelength of X-ray used (in nm), 'β' is the full width at half maximum (FWHM-in radian) and 'θ' is Bragg diffraction angle (in degree). The average crystallite size estimated to be 38 nm for undoped, 16 nm for Mn (0.5%), 13 nm for Mn

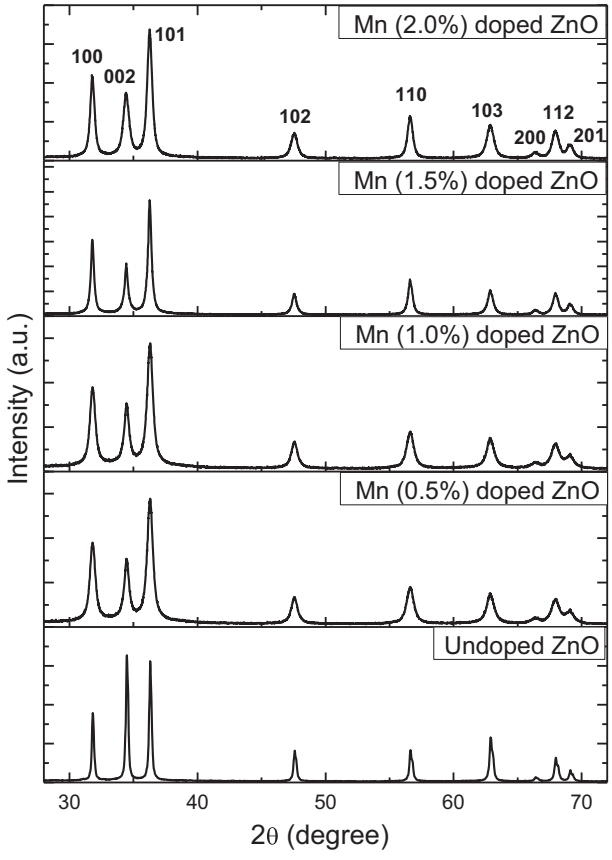

Fig. 1. XRD pattern of Mn (0.5–2.0%) doped and TG (1.0%) capped ZnO NPs.

(1.0%), 28 nm for Mn (1.5%) and 20 nm for Mn (2.0%) doped and TG (1.0%) capped ZnO NPs.

3.2. TEM

TEM micrographs of Mn (1.0%) doped and TG (1.0%) capped ZnO NPs synthesized at various pH values are shown in Fig. 2(a–d). It is clear from micrographs that Mn (1.0%) doped ZnO NPs at different pH have spherical morphology. Fig. 2(a) shows Mn (1.0%) doped ZnO NPs synthesized at pH-6.7 have agglomerated spherical shape particles with average particle size of 12–18 nm. Mn (1.0%) doped ZnO NPs synthesized at pH-8.0, 10.0 and 12.0 as shown in Fig. 2(b–d) also have agglomerated spherical particles with average particle size lying between 10 and 15 nm.

3.3. Optical properties

Optical absorption spectroscopy of prepared undoped and Mn (0.5–2.0%) doped ZnO NPs is performed by UV–Visible absorption spectroscopy at room temperature. Fig. 3(a) shows the absorption spectra of undoped and Mn (0.5–2.0%) doped ZnO NPs at natural pH i.e. at pH-6.7 and Fig. 3(b) shows the absorption spectra of Mn (1.0%) doped ZnO NPs at various pH values i.e. at pH-6.7 (natural pH), 8.0, 10.0 and 12.0. It can be seen from Fig. 3(a and b) that there is strong excitonic absorption peak for all as prepared samples. Fig. 3(a) shows the absorption peaks at 364 nm, 358 nm, 365 nm, 364 nm and 364 nm for undoped, Mn (0.5%), Mn (1.0%), Mn (1.5%) and Mn (2.0%) doped ZnO NPs respectively. Fig. 3(b) shows the absorption peak at 365 nm, 367 nm, 354 nm and 371 nm for Mn (1.0%) doped ZnO NPs at pH-6.7, 8.0, 10.0 and 12.0 respectively. These peaks in all samples are blue shifted in comparison to bulk ZnO having absorption peak at ~375 nm (Mahmood et al., 2011). All these blue shifted peaks attributed to large exciton binding energy and good optical quality of synthesized doped ZnO NPs. The weak absorption in all synthesized samples starts from 650 nm and becomes strong around 360 nm. The band gap has been calculated by using Tauc's formula which shows the relationship between absorption coefficient (α) and photon energy ($h\nu$) and can be written as:

$$\alpha h\nu = A(h\nu - E_g)^n \quad (2)$$

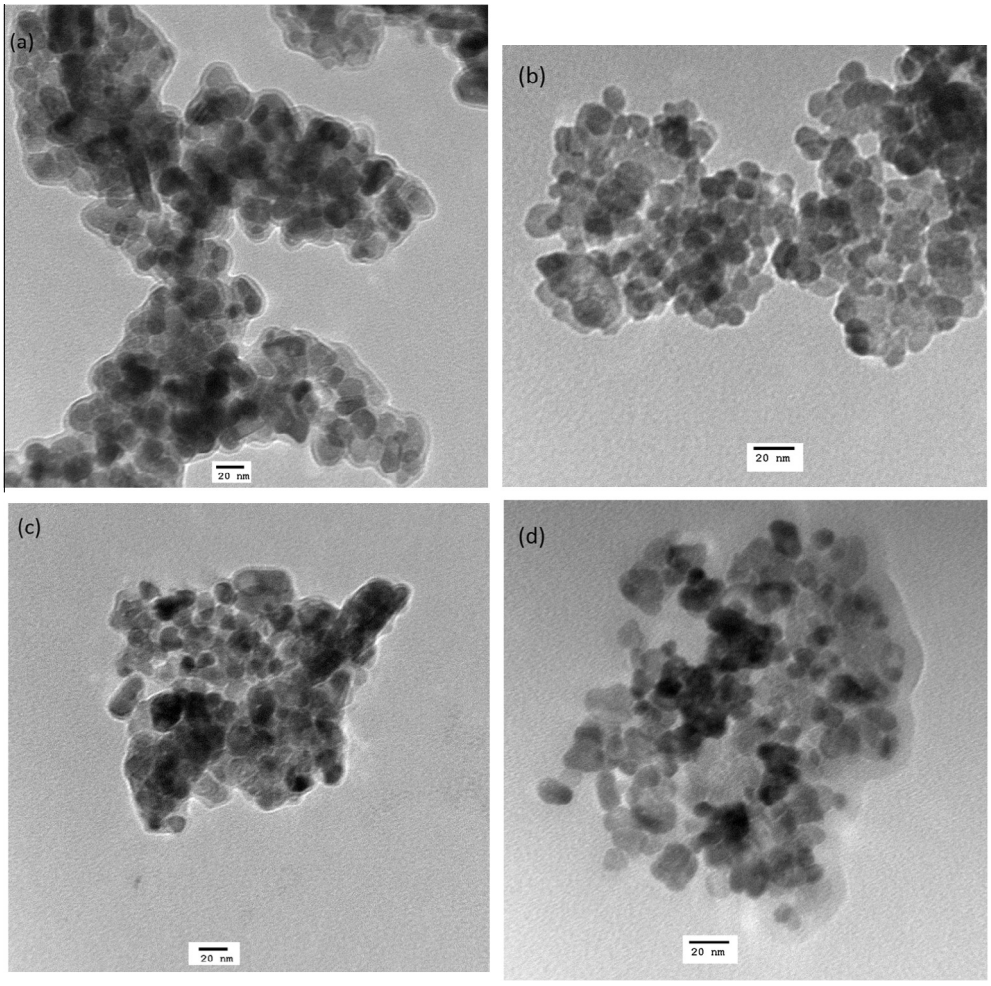

Fig. 2. TEM images of Mn (1.0%) doped ZnO NPs synthesized at (a) pH-6.7 (b) pH-8.0 (c) pH-10.0 and (d) pH-12.0.

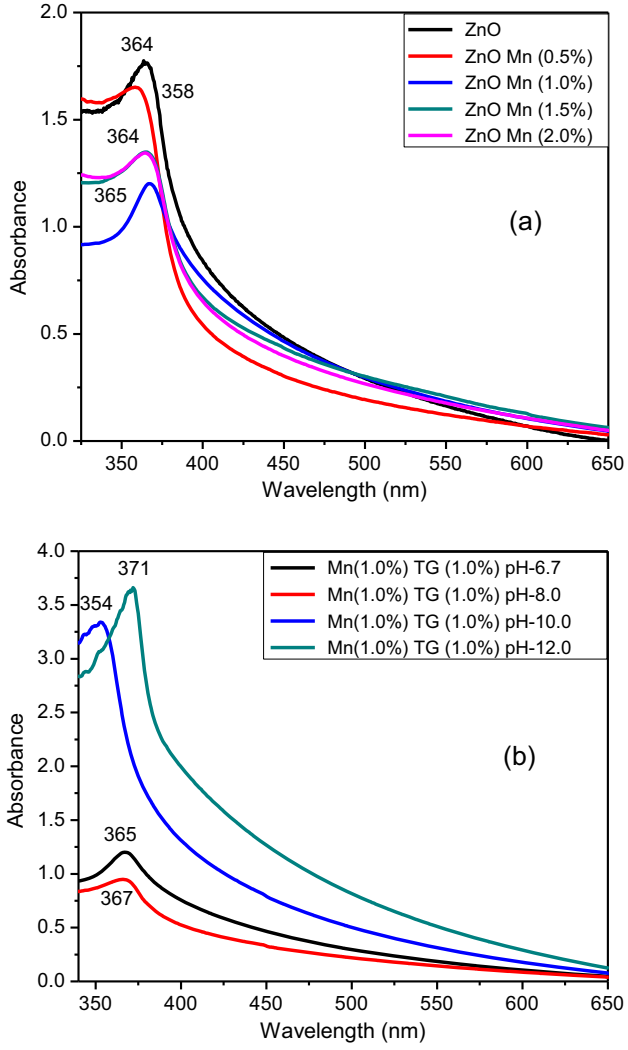

Fig. 3. UV–Visible absorption spectra of (a) Mn (0.5–2.0%) doped ZnO NPs (b) Mn (1.0%) doped ZnO NPs synthesized at different pH values.

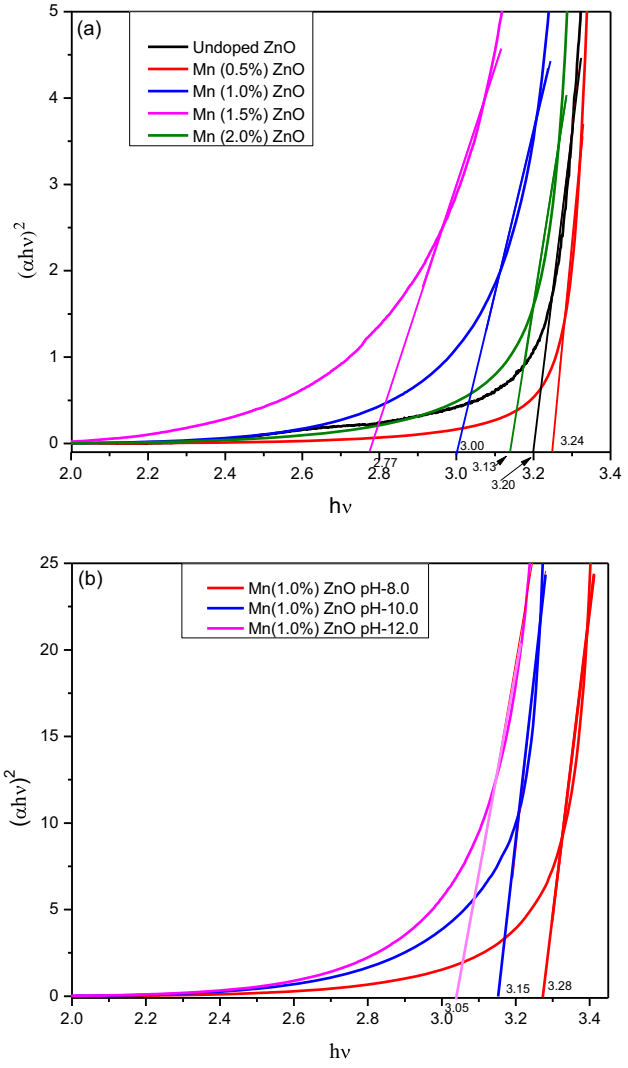

Fig. 4. Tauc's plot for (a) Mn (0.5–2.0%) doped ZnO at pH-6.7 and (b) Mn (1.0%) doped ZnO NPs synthesized at different pH values.

where 'A' is constant, 'α' is the absorption coefficient and n depends on the type of transition having values 1/2, 2, 3/2 and 3 corresponding to allowed direct, allowed indirect, forbidden direct and forbidden indirect respectively (Pankove, 1971). As ZnO has direct band gap so value of n is taken as 1/2. The band gap values has been determined by extrapolating the straight line portion of $(\alpha h\nu)^{1/n}$ versus $h\nu$ graph. Fig. 4(a and b) shows the graphs between $(\alpha h\nu)^2$ and $h\nu$ for undoped and Mn (0.5–2.0%) doped ZnO NPs at natural pH and Mn (1.0%) doped ZnO NPs synthesized at pH-6.7 (natural), 8.0, 10.0 and 12.0. The band gap values obtained are 3.20 eV, 3.24 eV, 3.00 eV, 2.77 eV and 3.13 eV for undoped, Mn (0.5%), Mn (1.0%), Mn (1.5%) and Mn (2.0%) doped ZnO NPs synthesized at pH-6.7 and 3.28 eV, 3.15 eV and 3.05 eV for Mn (1.0%) doped ZnO NPs synthesized at pH-8.0, 10.0 and 12.0 respectively. The band gap of doped ZnO NPs decreases as the doping concentration increases from 0.5% to 1.5%. This decrease in band gap of doped ZnO NPs is because the d-electron of Mn (t_{2g} levels) can easily overlap with ZnO valence band and this results in decrease in effective band gap (Halprin and Lax, 1966). So the photocatalyst's valence band gap can now be excited by visible light radiations. However, when Mn doping concentration increases to 2.0%, the band gap increases in comparison to other doped ZnO NPs and reaches to 3.13 eV which may be attributed to increase in doping concentration from optimum level as similar behavior has been observed in vanadium doped ZnO NPs (Tahir et al., 2009). This may be due to carrier concentration, structural parameter and defects due to oxygen vacancy which leads to Burstein Moss Shift (Chakraborty et al., 2003). Also, the band gap values calculated for doped NPs synthesized at pH-10.0 and 12.0 are significantly lesser than undoped ZnO NPs and thus may act as a better photocatalyst in UV–Visible light radiations (discussed later).

3.3.1. Excitation studies

Room temperature photoluminescence excitation spectra of undoped and Mn (1%) doped ZnO NPs monitored

at 468 nm emission are shown in Fig. 5. It has been found that undoped ZnO NPs shows broad excitation peak at 307 nm with small peak at 407 nm. In comparison to undoped ZnO NPs, Mn (1.0%) doped ZnO NPs shows sharp excitation peaks in UV region lying at 302 nm, 323 nm and 378 nm and one broad absorption peak in visible region at 439 nm. The broad absorption in between 370 and 450 nm comprises of three absorptions, assigned to $6A_{1g}(S) \rightarrow 4A_{1g}(G)$, $4E_g(G)$ and $6A_{1g}(S) \rightarrow 4\ T_{2g}(G)$ transition (Halprin and Lax, 1966). The broad absorption peak in visible region appear due to the energy levels created by Mn atom in the host ZnO NPs. The relative absorption intensities of Mn doped and undoped ZnO ($I_{\text{Mn doped/undoped}}$) are very high for the peaks considered around 307 nm and 439 nm. Thus PLE spectra show that energy levels have been created by impurity (Mn) atoms in the host ZnO samples therefore doped sample has better absorption in visible region as compared to undoped ZnO NPs.

3.3.2. Emission studies

Photoluminescence emission spectra of undoped and Mn (1.0%) doped ZnO NPs in powdered form which are synthesized at various pH values at 325 nm excitation is shown in Fig. 5(c). Inset of Fig. 5(c) shows magnified view of undoped ZnO NPs having strong emission peaks both in UV and Visible region. The UV emission mainly originates from near-band-edge (NBE) transitions in band gap of ZnO while the visible emission belongs to defect states such as impurities and oxygen vacancies in ZnO. On the other side Mn (1.0%) doped ZnO NPs synthesized at different pH shows very weak emission in UV region (380 nm) and strong emission in visible region (469 nm) along with small peaks at 532 and 612 nm. Emission intensity in UV region w.r.t. visible region in Mn doped NPs is very less as compared to undoped ZnO NPs. Thus incorporation of Mn ions into ZnO lattice leads to partial quenching of the band edge emission of ZnO. Mn doped II–VI nanomaterials generally emits fixed 590 nm emission due to well known d–d transitions [$6A_{1g}(S) \rightarrow 4\ T_{1g}(G)$] of Mn which lie in wide band gap of semiconductors (Sharma et al., 2010; Singh et al., 2015). In case of Mn doped ZnO NPs this well known 590 nm emission is absent. This has already been discussed in UV Visible absorption studies and earlier reports that d-states of Mn (t_{2g} levels) can easily overlap with ZnO valence band (V.B) and this results in quenching of 590 nm emission and results in decrease in effective band gap (Halprin and Lax, 1966). So overlap of one state (t_{2g}) of Mn with host V.B and presence of upper d state $6A_{1g}(S)$ in band gap helps to dissociate electron and hole wavefunction and decrease recombination. This is clear from PL studies that with doping both band edge (380 nm) of host ZnO decreases and d–d transitions (590 nm) of dopant Mn are absent. Weak blue emission lying at 469 nm can be due to the recombination of one d state $6A_{1g}(S)$ of Mn and defect states of ZnO host (Viswanatha et al., 2004). Fig. 5(d) shows at Mn (1.0%) doped NPs PL

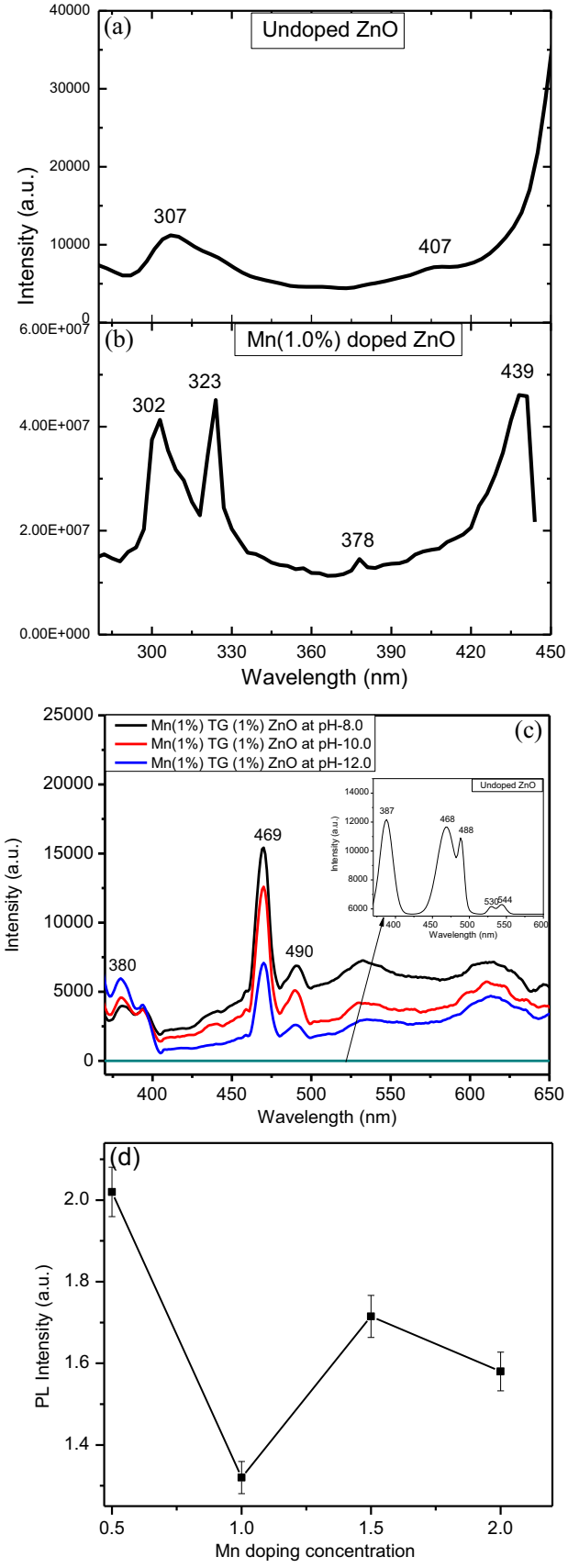

Fig. 5. PLE spectra of (a) Undoped and (b) Mn (1.0%) doped ZnO NPs at $\lambda_{em} = 468$ nm. PL spectra of (c) Mn (1.0%) doped ZnO NPs synthesized at pH-8.0, 10.0 and 12.0 at $\lambda_{ex} = 325$ nm and (d). Variation of Mn doping concentration with PL emission intensities.

emission intensity is minimum which suggests at this optimum doping concentration electron hole recombination is minimum. From Fig. 5(c) it can be observed that emission peak intensity of optimum doped NPs further decreased with increase in pH value from 8.0 to 12.0. This might be due to further reduction of recombination rate of electron and holes because Mn ions act as electron scavenger and increased pH helps to decrease recombination which is discussed in photocatalytic studies later.

3.4. Photocatalytic studies

Fig. 6(a) shows the histogram representing the variations of doping concentration with percentage degradation of CV for 1 h only. It shows under UV–Visible radiations 10.48%, 20.25%, 38.21, 66.10%, 42.26% and 52.35% of crystal violet has been degraded in 1 h without using any photocatalyst, using undoped NPs, Mn (0.5%, 1.0%, 1.5% and 2.0%) doped ZnO NPs as a different photocatalyst respectively. Thus maximum degradation has been achieved by Mn (1.0%) doped ZnO NPs. For complete degradation studies, the photocatalytic activity of as synthesized undoped, Mn (1%) doped and Mn (2%) doped ZnO NPs were evaluated by degradation of CV dye molecules under UV–Visible irradiations because of their better photocatalytic activity in 1 h. This dye was used as a test contaminant owing to its absorption peaks in visible range and its degradation can be easily monitored by optical absorption spectroscopy. The changes in optical absorption spectra of CV dye with undoped and Mn (1.0%) doped ZnO NPs synthesized at pH-6.7 is shown in Fig. 6(b and c). The spectra have been taken after 30 min. intervals after exposing the solution under UV–Visible light. The intensity of absorption spectra decreases as the exposing time increases from 0 to 3 h. The intensity of main peak lying at 589 nm decreases due to degradation of CV dye. Fig. 7 (a) shows the change in concentration of CV dye as a function of irradiation time for the dye derivatives in absence and presence of undoped, Mn (1.0%) and Mn (2.0%) doped ZnO NPs. Here 'C' is the concentration of CV determined at λ_{max} of absorption and 'C_0' is initial concentration. Fig. 7(b) shows the percentage degradation of CV dye under different conditions. It shows that 22% of CV dye dissolved in water disappears in 3 h of UV–Visible radiations in the absence of any photocatalyst. This smaller degradation of CV dye might be due to the interaction between $OH^{\cdot}$ radical generated from water molecules and CV dye. 40% of CV dye has been degraded with undoped ZnO NPs. Photocatalytic activity of undoped ZnO NPs are due to defect states caused by donor and acceptor states such as oxygen vacancies, interstitial zinc atom and zinc vacancies and interstitial oxygen respectively. Interfacial electron transfer takes place between donor state and CV dye. As CV dye is cationic in nature so it acquire electron from donor excited state and get decomposed. Fig. 7(b) shows 92.6% and 69.7% of CV dye degraded with Mn (1.0%) and Mn (2%) doped ZnO NPs synthesized at pH-6.7 when exposed to UV–Visible light radiations for 3 h. Thus photocatalyst is necessary for photocatalytic reaction. Mn doped ZnO samples has shown better

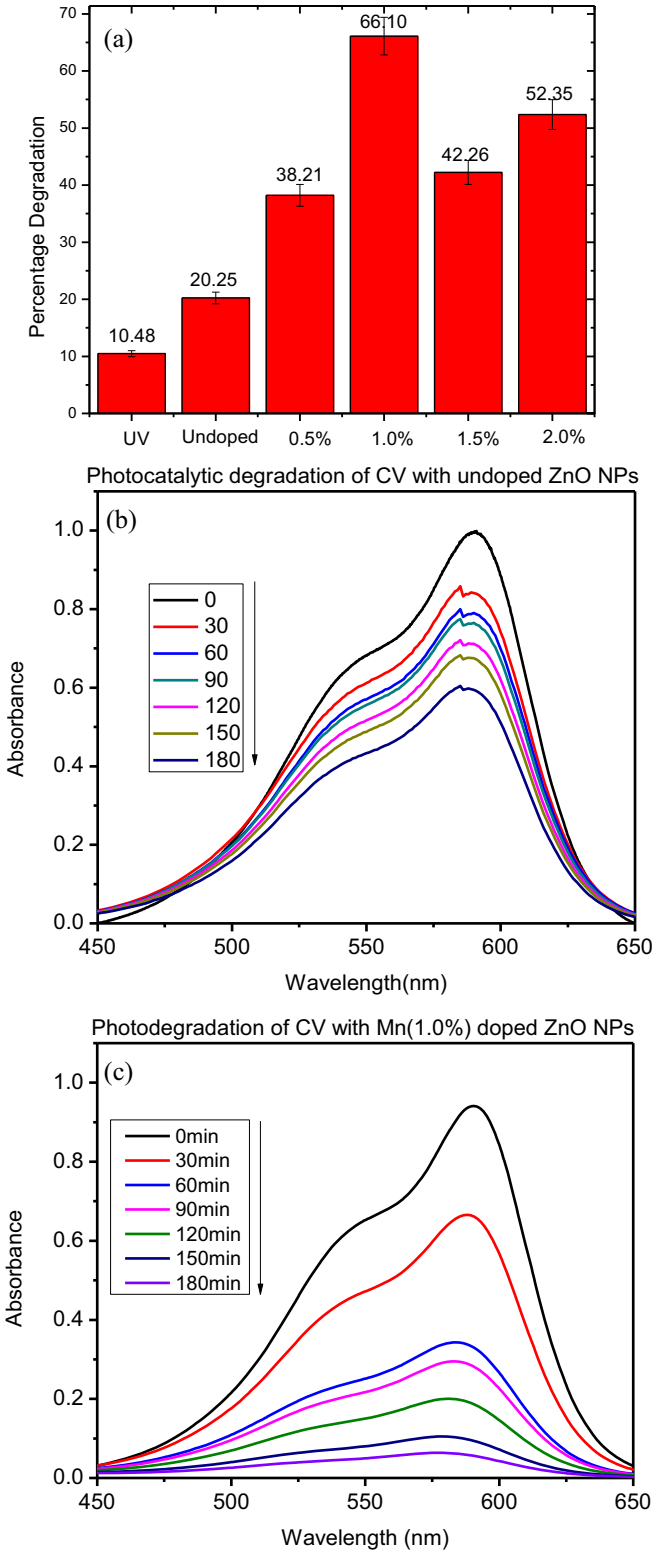

Fig. 6. (a) Histogram for percentage degradation of CV dye at different conditions under UV–Visible radiations for 1 h. Change in optical absorption spectra of CV dye aqueous solution (10 mg/L) with (b) undoped and (c) Mn (1.0%) doped ZnO NPs.

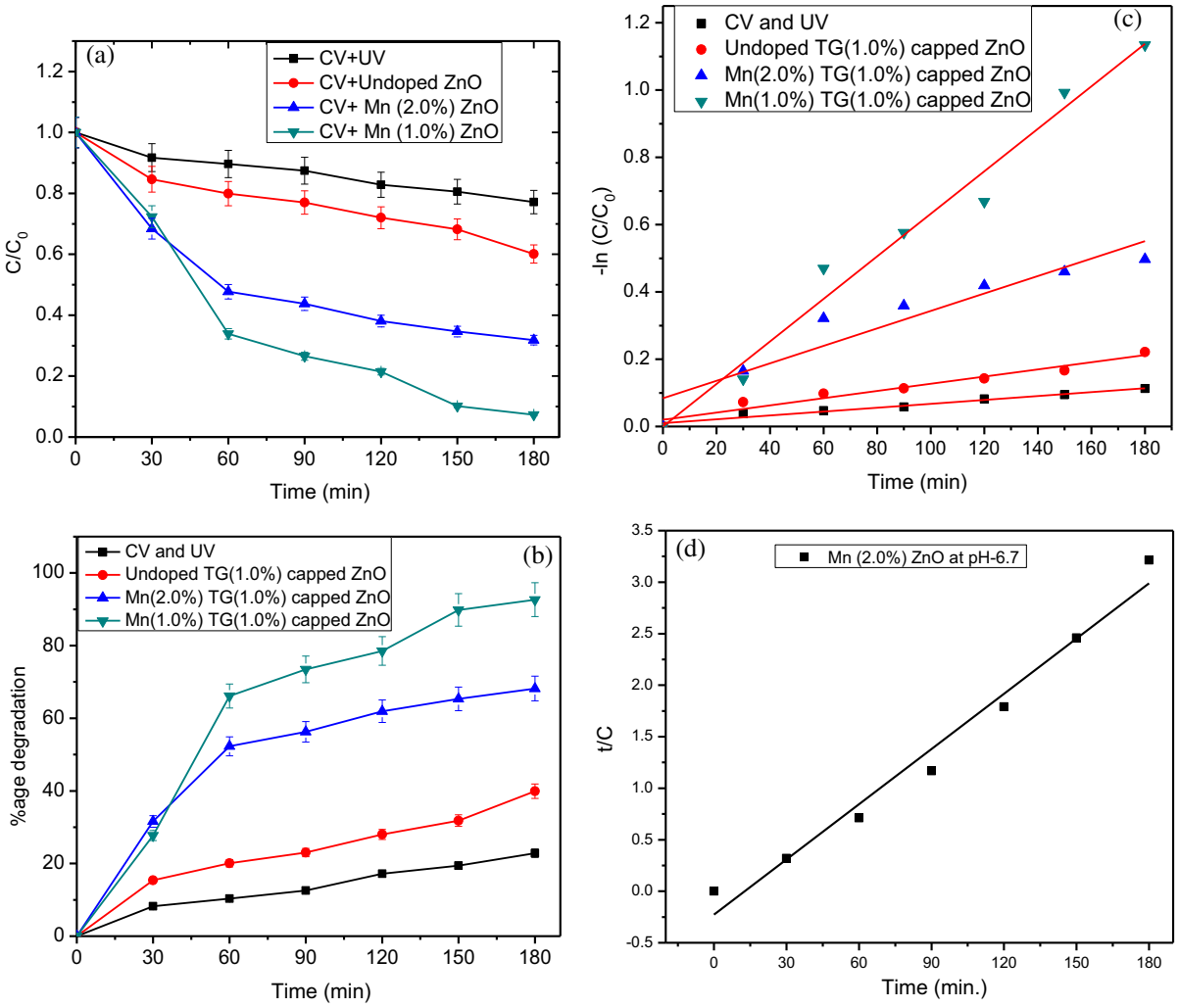

Fig. 7. (a) Photodegradation of CV under different conditions (b) extent of decomposition of CV dye with respect to time intervals (c) first order kinetics of crystal violet degradation with and without photocatalyst and (d) second order kinetics of CV degradation Mn (2.0%) doped ZnO NPs synthesized at pH-6.7 under UV–Visible radiations.

degradation as compare to undoped ZnO NPs. As discussed earlier in excitation and emission spectroscopy studies Mn doping in ZnO NPs modify the energy band of ZnO, through the creation of localized Mn dopant energy levels within the bandgap. Under UV–Visible light illumination, the photogenerated electrons could easily transfer from the VB of ZnO to the localized Mn energy levels, along with the d–d transitions between the Mn dopant energy levels. The excited electrons were readily trapped in these Mn dopant sites, while the photogenerated holes were left in the valence band of ZnO and migrated to the surface of doped NPs, yielding active hydroxyl radical species to decompose the CV dye. As discussed above in excitation and emission studies there is considerable shift in excitation and emission spectra by addition of Mn dopant ions in host ZnO NPs. Therefore the incorporation of Mn dopant ions in ZnO NPs act as effective trapping sites. The photogenerated electrons and holes can be efficiently separated and the recombination of these charge carriers has been greatly inhibited which results in the improved photocatalytic activities (Yang et al., 2013). Mn (1.0%) doped ZnO NPs has shown better photocatalytic activity than Mn (2.0%) doped ZnO sample. It may be due to smaller particle size (confirmed from XRD) as compared to Mn (2.0%) doped ZnO photocatalyst. The surface to volume ratio for Mn (1.0%) doped ZnO NPs is higher and activity of photocatalyst depends upon the adsorption amount of dye molecules on the surface of the photocatalyst. Also the effective band gap of Mn (1.0%) doped ZnO sample is smaller than Mn (2.0%) doped ZnO NPs (discussed earlier). This also increases the photocatalytic efficiency of Mn (1.0%) doped ZnO sample under exposure of UV–Visible light radiations. The photocatalytic decomposition of CV dye on the surface of ZnO NPs follows a pseudo first and second-order kinetic law, which can be expressed by following equations as,

$$-\ln(C/C_0) = K_1 t \tag{3}$$

$$t/C = 1/K_2 C_0^2 + t/C_0 \tag{4}$$

where C and C_0 are the reactant concentration at time $t = t$ and $t = 0$, respectively. K_1, K_2 and t are the pseudo-first and second-order rate constants (reaction rate constant) and time, respectively (Fujishima et al., 2000; Gusain et al., 2014). The relationship between $-\ln(C/C_0)$ and irradiation time (Reaction time) for first order and t/C and irradiation time for second order are shown in Fig. 7(c and d) respectively. Rate constants (K_1 and K_2) and regression coefficient (R) for degradation of CV dye with and without catalysts are summarized in Table 1. It shows that Mn (2.0%) doped ZnO NPs follows second order kinetics. Also the photoreaction rate is highest for Mn (1.0%) doped ZnO NPs and is least for CV dye under UV–Visible radiations only. This shows that Mn (1.0%) doped ZnO NPs shows highest photocatalytic performance among all synthesized photocatalysts.

3.5. Effect of pH on photocatalysis

Since the waste water from textile industries have wide range of pH values and it is very difficult to study the pH of waste water from industries at each time and adjust the photocatalytic reaction. To optimize the type of photocatalyst according to waste water pH, many groups have studied the effect of pH by varying the pH of dye solution with addition of acids and bases (Ji et al., 2009; Kong et al., 2010). We first time synthesized Cu doped ZnO NPs at variable pH and thus optimize the pH of photocatalyst to degrade dye of any pH values (Mittal et al., 2014). Thus, with this system there is no need to study the pH of effluents from industries. Since till now no one has synthesized Mn doped ZnO NPs at variable pH and studied their effect on photodegradation of dyes, so attempts have been made to optimize doping and pH of Mn doped ZnO NPs during synthesis of NPs to achieve maximum degradation of dye under UV–Visible light radiations. At this point it is important to mention that pH of photocatalytic reaction is constant (neutral) in all experiments with samples having different pH during synthesis of NPs. But they show considerable effect of photocatalytic reaction. As Mn (1.0%) doped ZnO NPs synthesized at pH-6.7 (natural) exhibit higher percentage of photodegradation of CV dye, therefore this category of sample has been selected for further study by varying the pH so that both doping and pH effect can be studied simultaneously. Mn (1.0%) doped ZnO NPs have been synthesized at pH 8.0, 10.0 and 12.0 to study the effect of pH on photocatalytic degradation studies. Fig. 8 (a) shows the decrease in concentration of CV dye when exposed to UV–Visible radiations in the presence of Mn (1.0%) doped ZnO NPs prepared at pH-8.0, 10.0 and 12.0. Percentage degradation of CV dye under similar conditions is shown in Fig. 8(b). It indicates that 95% and 98.3% CV dye has been degraded with Mn (1.0%) doped ZnO NPs at pH-8.0 and 10.0 respectively in 3 h of UV–Visible exposure of radiations. However, 99.8% of CV dye has been degraded with Mn (1.0%) doped ZnO NPs synthesized at pH-12 after 2.5 h of exposure of UV–Visible radiations. Thus higher degree of CV dye degradation has been obtained at higher pH value at lower irradiation time. The linear relationship between $-\ln(C/C_0)$ and irradiation time for first order and t/C and irradiation time for second order is shown in Fig. 8(c and d) respectively. The pseudo-first-order rate constant (K) and regression coefficient (R) for degradation of CV dye with Mn (1.0%) doped ZnO NPs at different pH valued are summarized in Table 1. The zero point charge of ZnO (pH_{zpc}) has been reported to be 9.0 (Zhao et al., 1998) and the surface functional groups of ZnO are $ZnOH_2^+$, ZnOH and ZnO^- at $pH < pH_{zpc}$, pH_{zpc} and $pH > pH_{zpc}$ respectively. As zero point charge (pH_{zpc}) of ZnO is 9.0, so at pH-10.0 ($pH > pH_{zpc}$) ZnO surface is anionic in nature which is further more anionic at pH-12.0 and CV dye is cationic in nature, so there is weak interaction, normal interaction and strong interactions between CV dye and Mn (1.0%) doped NPs synthesized at pH 8.0, 10.0 and 12.0 respectively. Therefore, greater dye molecule will adsorb on photocatalyst surface at pH-12.0 than at pH-8.0 and 10.0. Also higher photodegradation efficiency at higher pH is due to the main reaction presented by hydroxyl radical attack, which can be highly favored by the high concentration of adsorbed hydroxyl

Table 1
Reaction rate constant of crystal violet without catalyst, undoped, Mn (1.0%, and 2.0%) doped and TG (1.0%) capped ZnO NPs synthesized at pH-8.0, 10 and 12.0.

S. no.	Concentration of CV (mg/L)	Catalyst type	pH of photocatalyst	Pseudo-first order		Pseudo-second order	
				Rate of reaction (K_1)	R^2	Rate of reaction (K_2)	R^2
1	10	No catalyst	–	0.00057	0.9669	–	–
2	10	Undoped ZnO	6.7	0.00107	0.9477	–	–
3	10	Mn (1.0%) ZnO	6.7	0.00631	0.9756	–	–
4	10	Mn (2.0%) ZnO	6.7	0.0026	0.8788	0.0016	0.9779
5	10	Mn (1.0%) ZnO	8.0	0.01613	0.9297	–	–
6	10	Mn (1.0%) ZnO	10.0	0.02125	0.9330	–	–
7	10	Mn (1.0%) ZnO	12.0	0.02494	0.8852	0.0186	0.9728
8	10	No catalyst H_2O_2	–	0.01385	0.9854	–	–
9	10	Mn (1.0%) ZnO H_2O_2	8.0	0.09493	0.8485	0.0015	0.90651
10	10	Mn (1.0%) ZnO H_2O_2	10.0	0.09955	0.9761	–	–
11	10	Mn (1.0%) ZnO H_2O_2	12.0	0.20064	0.9377	–	–

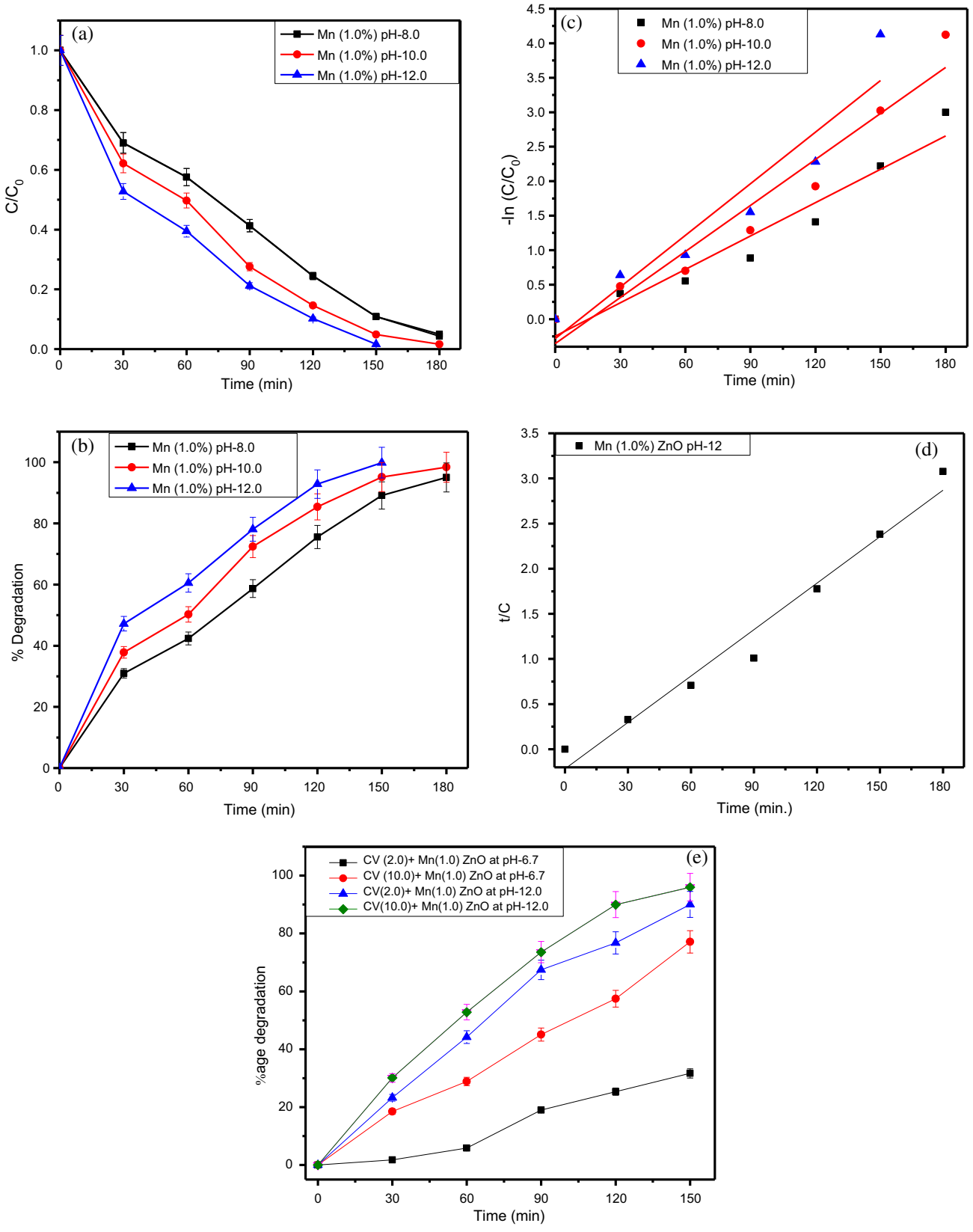

Fig. 8. (a) Photodegradation of CV dye (b) extend of decomposition of CV dye (c) first order kinetics of CV degradation with Mn (1.0%) doped ZnO NPs synthesized at pH-8.0, 10.0 and 12.0. (d) Second order kinetics of CV degradation with Mn (1.0%) doped ZnO NPs at pH-12.0 and (e) extend of decomposition of CV dye solution at pH-2.0 and 10.0 with Mn (1.0%) doped ZnO NPs synthesized at pH-6.7 and 12.0.

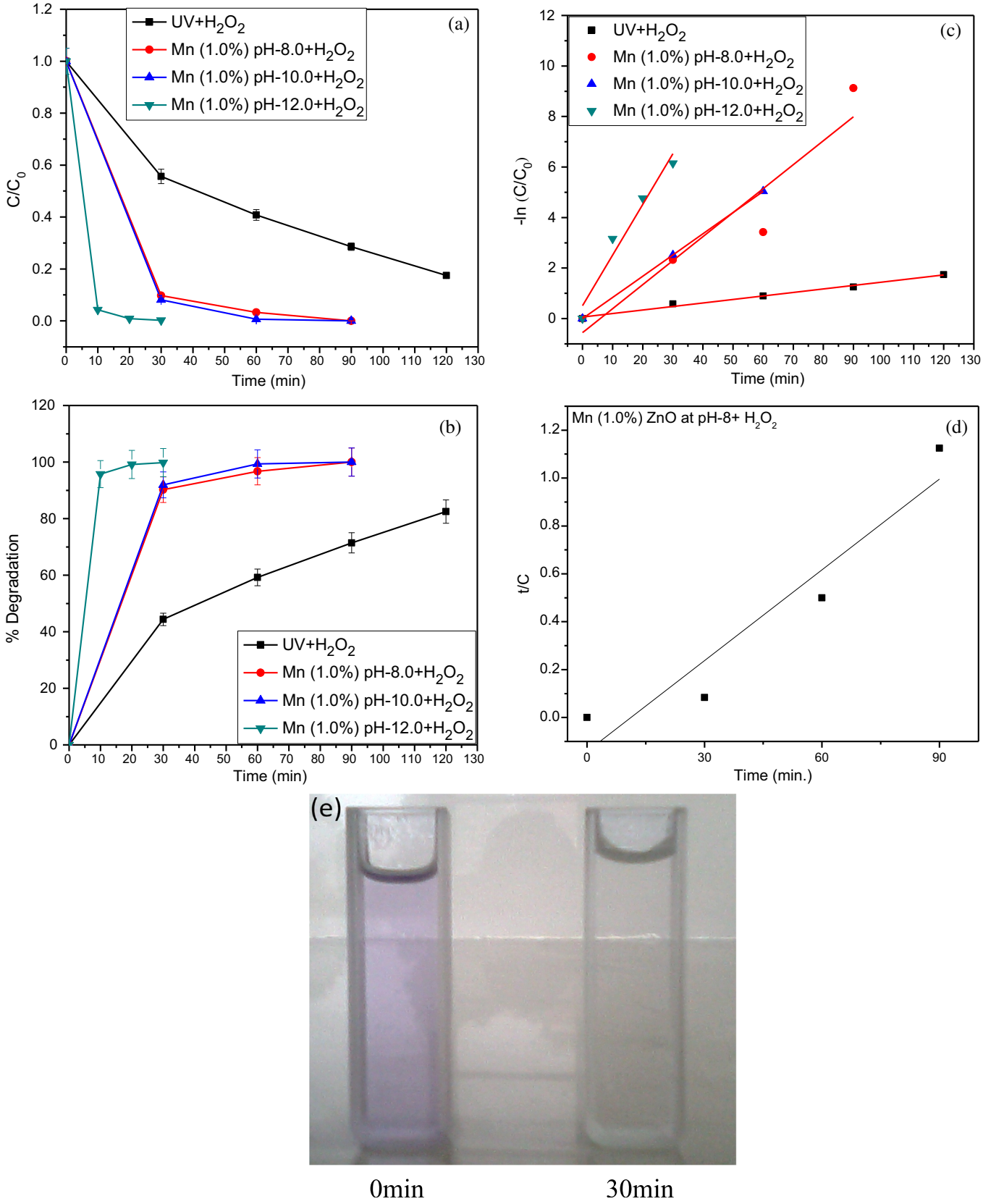

Fig. 9. (a) Change in concentration (b) percentage degradation and (c) first order kinetics of degradation of CV dye under the exposure of UV–Visible light radiations with and without synthesized photocatalyst at different pH values (d) second order kinetics of CV dye with Mn (1.0%) doped ZnO at pH-8.0 in the presence of in the presence of H_2O_2 and (e) change in color of CV dye with Mn (1.0%) doped ZnO NPs synthesized at pH-12 in the presence of H_2O_2 under UV–Visible light radiations after 0 mins and 30 mins. (For interpretation of the references to colour in this figure legend, the reader is referred to the web version of this article.)

groups at high pH values (Gouvea et al., 2000). Further to check the photodegradation efficiency of as synthesized Mn (1.0%) doped ZnO NPs at pH-12.0, the CV dye solution has been prepared at pH-2.0 (acidic medium) and 10.0 (basic medium) with the addition of HNO_3 and NaOH. The CV solution at pH-2.0 and 10.0 has been degraded with Mn (1.0%) doped ZnO NPs synthesized at pH-6.7 and 12.0. Fig. 8(e) shows the percentage degradation of CV dye solution at different pH values under UV–Visible light in the presence of Mn (1.0%) doped ZnO NPs synthesized at pH-6.7 and 12.0. It shows that the 31.6% and 77% CV dye solution at pH-2.0 and 10.0 has been degraded with Mn (1.0%) doped ZnO NPs synthesized at pH-6.7 and 90.4% and 96.0% CV dye has been degraded with Mn (1.0%) doped ZnO NPs synthesized at pH-12.0 in 150 min of UV–Visible light radiations. Thus Mn doped ZnO sample synthesized at pH-12.0 has efficiently degraded the CV dye in acidic, neutral and basic medium. These results confirm the utility of these NPs for degradation of waste water effluents from industries.

3.6. Effect of H_2O_2 on photocatalysis

As discussed above, doping and pH has dominant effect on photocatalysis of CV dye. In order to further enhance the degradation rate, the effect of H_2O_2 has been investigated so that effect of doping, pH and H_2O_2 could be studied simultaneously. The minimum amount of H_2O_2 (1.0%) has been added to 100 mL slurry solution (dye and ZnO nanopowder). Fig. 9(a) shows decrease in concentration of CV dye when exposed to UV–Visible light in the presence of H_2O_2 along with and without Mn (1.0%) doped ZnO NPs synthesized at different pH values. Percentage degradation of CV dye under similar conditions is shown in Fig. 9(b). It shows that more than 82% of CV dye has been degraded in 2 h with H_2O_2 only under UV–Visible radiations. More than 90% and almost 100% CV dye has been degraded in 1.5 h in the presence of Mn (1.0%) doped ZnO NPs synthesized at pH-8.0 and 10.0 respectively. However very quick degradation has been observed with Mn (1.0%) doped ZnO NPs synthesized at pH-12 along with H_2O_2. It has been found that 99% dye has been degraded in 20 min. and 100% CV dye has been degraded 30 min. respectively. The linear relationship between $-\ln(C/C_0)$ and irradiation time for first order and t/C and irradiation time for second order is shown in Fig. 9(c and d). The pseudo-first and second-order rate constants and regression coefficients (R) for degradation of CV dye in the presence of H_2O_2 without and with Mn (1.0%) doped ZnO NPs at different pH valued are summarized in Table 1. The photoreaction rate is higher for Mn (1.0%) doped ZnO NPs synthesized at pH-12.0 as compared to others. Change in color of CV dye using Mn (1.0%) doped ZnO NPs synthesized at pH-12.0 in the presence of H_2O_2 for 0 min and 30 min under UV–Visible light radiations is shown in Fig. 9 (d). It shows that color of CV dye has been changed from violet to colorless after 30mins. This change in color shows

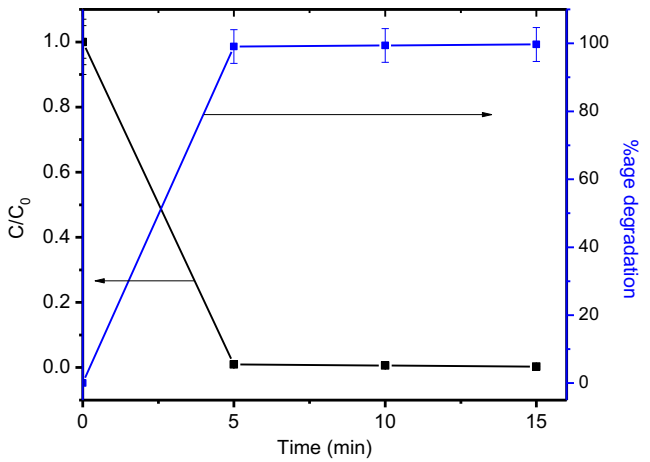

Fig. 10. Change in concentration and percentage degradation of Sirius red F3B dye using Mn (1.0%) doped ZnO NPs at pH-12.0 in the presence of H_2O_2 under UV–Visible light radiations.

that dye has been degraded. The degradation of CV dye with H_2O_2 only is due to direct photocatalysis of H_2O_2 by UV–Visible light radiations that can generate free radicals. Also H_2O_2 is suggested to be better electron acceptor than oxygen. As hydroxyl radicals are strong oxidizing agents and hence play significant role in degradation of dyes.

So in Mn (1.0%) doped ZnO NPs, Mn reduces electron–hole recombination which help H_2O_2 to generate higher amount of hydroxyl radicals. Also pH plays significant role for producing strong oxidizing agents. Therefore this two way process generate strong oxidizing agents causes faster degradation of CV dye in the presence of photocatalysts synthesized at different pH values. Thus doping, pH and presence of H_2O_2 appears to be promising factors for quick degradation of CV dye.

Further to check the photocatalytic activity of Mn (1.0%) doped ZnO NPs at pH-12.0 in the presence of H_2O_2, anionic industrial polyazo Sirius red F3B (SRF3B) dye has been degraded. Change in concentration and percentage degradation of SRF3B dye has been shown in Fig. 10. It indicates very fast and quick degradation of SRF3B dye under UV–Visible light radiations. 100% degradation of SRF3B dye has been achieved within 15mins under exposure of UV–Visible light radiations. Thus highly efficient photocatalyst has been synthesized for degradation of both cationic and anionic dyes in industrial effluents to reduce water pollution and to save aquatic life.

4. Conclusion

Undoped and Mn doped and TG capped ZnO NPs were synthesized by co-precipitation route initially at pH-6.7. XRD pattern confirm the formation of doped ZnO samples without any secondary phase appearance. PLE spectra have shown large absorption in visible region as compared

to undoped NPs. PL emission and excitation spectra showed that incorporation of Mn ions in NPs have decreased electron–hole recombination. Photocatalytic studies shows that Mn (1.0%) doped ZnO NPs synthesized at pH-6.7 to be better photocatalyst when exposed to UV–Visible light radiations for 1 h only. 92% CV dye has been degraded using Mn (1.0%) doped ZnO NPs synthesized at pH-6.7 after 3.0 h of UV–Visible radiations. Similarly Mn doped ZnO samples synthesized at pH-8.0 and 10.0 have shown 95% and more than 98% degradation of CV dye under similar conditions. When pH of the as synthesized Mn (1.0%) doped ZnO samples were raised to 12.0, almost 100% CV dye has been degraded in 2.5 h only. Mn (1.0%) doped ZnO photocatalyst synthesized at pH-12.0 has also efficiently degraded the CV dye at pH-2.0 and 10.0 as compared to similar doped sample synthesized at pH-6.7. Further fast and quick CV dye degradation has been observed when only 1.0% of H_2O_2 added during photocatalytic reaction. As compared to 82% degradation of CV dye with H_2O_2 only in 2 h without any photocatalyst under UV–Visible radiations, 100% CV dye has been degraded in 90mins with Mn (1.0%) doped ZnO NPs synthesized at pH-8.0 and 10.0 in the presence of H_2O_2. However, Mn (1.0%) doped ZnO NPs synthesized at pH-12.0 has shown highest degradation reaction rate of CV dye and has degraded more than 99% dye in 20 mins and 100% dye in 30 mins only in the presence of H_2O_2. To check the utility of highly efficient photocatalyst for anionic dyes also in industries, degradation of polyazo Sirius red F3B (SRF3B) industrial dye has been studied and 100% degradation has been achieved in 15mins of UV–Visible light radiations only. This means doping, pH and presence of H_2O_2 all have shown significant contribution for quick degradation of dye. With this system industrial effluents with any pH value can be degraded quickly and thus to save aquatic life.

References

Akpan, U.G., Hameed, B.H., 2009. Parameters affecting the photocatalytic degradation of dyes using TiO_2 – based photocatalysts: a review. J. Hazard. Mater. 70, 520–529.

Akyol, A., Bayramoglu, M., 2005. Photocatalytic degradation of Remazol Red F3B using ZnO catalyst. J. Hazard. Mater. B124, 241–246.

Behnajady, M.A., Modirshahla, N., Hamzavi, R., 2006. Kinetic study on photocatalytic degradation of C.I. Acid Yellow 23 by ZnO photocatalyst. J. Hazard. Mater. 133, 226–232.

Bhosale, R.R., Pujari, S.R., Muley, G.G., Patil, S.H., Patil, K.R., Shaikh, M.F., Gambhire, A.B., 2014. Solar photocatalytic degradation of methylene blue using doped TiO_2 nanoparticles. Solar Energy 103, 473–479.

Chakraborty, P.K., Dutta, G.C., Ghatak, K.P., 2003. A simple theoretical analysis of the effective electron mass in heavily doped lll–V semiconductor in the presence of band-tails. Phys. Scripta 68, 368.

Chandran, P., Kumari, P., Khan, S.S., 2014. Photocatalytic activation of CdS NPs under visible light for environmental cleanup and disinfection. Solar Energy 105, 542–547.

Chio, W., Termin, A., Hoffmann, M.R., 1994. The role of metal ion dopants in quantum- sized TiO_2: correlation between photoreactivity and charge carrier recombination dynamics. J. Phys. Chem. 98, 13669–13679.

Donkova, B., Dimitrov, D., Kostadinov, M., Mitkova, E., Mehandjiev, D., 2010. Catalytic and photocatalytic activity of lightly doped catalysts M:ZnO (M = Cu, Mn). Mater. Chem. Phys. 123, 563–568.

Fujishima, A., Rao, T.N., Tryk, D.A., 2000. Titanium dioxide photocatalysis. J. Photochem. Photobio. C: Photochem. Rev. 1, 1–21.

Gouvea, C.A.K., Wypych, F., Moraes, S.G., Duran, N., Nagata, N., Zamor, P.P., 2000. Semiconductor-assisted photocatalytic degradation of reactive dyes in aqueous solution. Chemosphere 40, 433–440.

Gusain, D., Upadhyay, S.N., Sharma, Y.S., 2014. Adsorption of Orange G dye on nano zirconia: error analysis for achieving the best equilibrium and kinetic modeling. RSC Adv. 4, 18755–18762.

Halprin, B., Lax, M., 1966. Impurity-band tails in the high density limit. l. Minimum counting methods. Phys. Rev. 148, 722.

Ji, P., Zhang, J., Chen, F., Anpo, M., 2009. Study of adsorption and degradation of acid orange 7 on the surface of CeO_2 under visible light irradiation. Appl. Catal. B: Environ. 85, 148–154.

Kamat, P.V., 2002. Photo-induced transformations in semiconductor–metal nanocomposite assemblies. J. Appl. Chem. 74, 1693–1706.

Kislov, N., Lahiri, J., Verma, H., Goswami, D.Y., Stefanakos, E., Batzill, M., 2009. Photocatalytic degradation of methyl orange over single crystalline ZnO: orientation dependence of photoactivity and photostability of ZnO. Langmuir 25, 3310–3315.

Klosek, S., Raftery, D., 2001. Visible light driven V-doped TiO_2 photocatalyst and its photo-oxidation of ethanol. Phys. Chem. B 105, 2815–2819.

Kong, J.Z., Li, A.D., Li, X.Y., Zhai, H.F., Zhang, W.Q., Gong, Y.P., Li, H., Wu, D., 2010. Photo-degradation of methylene blue using Ta doped ZnO nanoparticle. J. Sol. State Chem. 183, 1359–1364.

Lima, C.S., Batista, K.A., Rodriguez, A.C., Souza, R.J., Fernandes, F.K., 2015. Photodecomposition and color removal of a real sample of textile wastewater using heterogeneous photocatalysis with polypyrrole. Solar Energy 114, 105–113.

Mahmood, M.A., Baruah, S., Dutta, J., 2011. Enhanced visible light photocatalysis by manganese doping or rapid crystallization with ZnO nanoparticles. Mater. Chem. Phys. 130, 531–535.

Martin, S.T., Morrison, C.L., Hoffmann, M.R., 2004. Photochemical mechanism of size-quantized vanadium-doped TiO_2 particles. J. Phys. Chem. 98, 13695–13704.

Milenova, K., Stambolova, I., Blaskov, V., Eliyas, A., Vassilev, S., Shipochka, M., 2013. The effect of introducing Cu dopant on the photocatalytic activity of ZnO nanoparticles. J. Chem. Technol. Metal. 48 (3), 259–264.

Mittal, M., Sharma, M., Pandey, O.P., 2014. UV–Visible light induced photocatalytic studies of Cu doped ZnO nanoparticles prepared by co-precipitation method. Solar Energy 110, 386–397.

Pankove, J.I., 1971. Optical Processes in Semiconductors. Prentice-Hall, Englewood Cliffs, NJ.

Poulios, I., Makri, D., Prohaska, X., 1999. Photocatalytic treatment of olive milling waste water, oxidation of protocatechuic acid, Global nest. Int. J. 1, 55–62.

Rehman, S., Ullah, R., Butt, A.M., Gohar, N.D., 2009. Strategies of making TiO_2 and ZnO visible light active. J. Hazard. Mater. 170, 560–569.

Sharma, M., Jain, T., Singh, S., Pandey, O.P., 2012. Photocatalytic degradation of organic dyes under UV–Visible light using capped ZnS nanoparticles. Solar Energy 86, 626–633.

Sharma, M., Kumar, S., Pandey, O.P., 2010. Excitation induced tunable emission in biocompatible chitosan capped ZnS nanophosphores. J. Appl. Phys. 107, 104319.

Singh, A., Kaur, R., Pandey, O.P., Wei, X., Sharma, M., 2015. Synthesis of fluorescent core-shell nanomaterials and strategies to generate white light. J. Appl. Phys. 118, 044305.

Tahir, N., Hussain, S.T., Usman, M., Husanain, S.K., Mumtaz, A., 2009. Effect of vanadium doping on structural, magnetic and optical properties of ZnO nanoparticles. Appl. Surf. Sci. 255, 8506–8510.

Viswanatha, R., Sapra, S., Gupta, S.S., Satpati, B., Satyam, P.V., Dev, B.N., Sarma, D.D., 2004. Synthesis and characterization of Mn-doped ZnO nanocrystals. J. Phys. Chem. B 108, 6303–6310.

Wang, X.L., Luan, C.Y., Shao, Q., Pruna, A., Leung, C.W., Lortz, R., Zapien, J.A., Ruotolo, A., 2013. Effect of the magnetic order on the room-temperature band-gap of Mn-doped ZnO Thin films. Appl. Phys. Lett. 102, 102112.

Yang, Y., Li, Y., Zhu, L., He, H., Hu, L., Huang, J., Hu, F., He, B., Ye, Z., 2013. Shape control of colloidal Mn doped ZnO nanocrystals and their visible light photocatalytic properties. Nanoscale 5, 10461–10471.

Zhao, J., Wu, T., Wu, K., Oikawa, K., Hidaka, H., Serpone, N., 1998. Photoassisted degradation of dye pollutants. 3. Degradation of the cationic dye rhodamine B in aqueous anionic surfactant/TiO_2 dispersion under visible light irradiation: evidence for the need of substrate adsorption on TiO_2 particles. Environ. Sci. Technol. 32, 2394–2400.